

# Accuracy Verification of Visual Appearance Acquisition Device of Non-Metallic Material Based on Sparse SVBRDF

Tsung-Lin Lu, Yu-Lun Liu, Yu-Cheng Hsieh, Tzung-Han Lin

National Taiwan University of Science and Technology, Taiwan

Keywords: Visual appearance, Spatially Varying Bidirectional Reflectance Distribution Function, Cook-Torrance Model.

## ABSTRACT

In this paper, we proposed a visual appearance acquisition device comparing with commercial product. Our device is capable of restoring the visual appearance for non-metallic materials based on spatially varying bidirectional reflectance distribution function (SVBRDF). A benchmark comparing to commercial product Radiant Vision is carried out to verify the reliability of the proposed device.

## 1 INTRODUCTION

How to accurately obtain the visual experience of materials has become an important issue. Nowadays, to increase the value of industrial products, CMF (Color Material Finish) needs more accurate material characteristics. To solve this problem, CIE (Commission Internationale de'Eclairage) already defined visual appearance in 2008 [1]. In general, visual appearance consists of the properties of color, texture, gloss, and transparency that are evaluated by the approach of quantitative analysis.

### 1.1 Background

In recent years, photo-realistic rendering in virtual reality is getting more and more attraction. Many researches, such as B. Burley [2], C. Hery, R. Villemin, and P. Studios [3], A. Pranckevičius [4], and S'ebastien Lagarde, Charles de Rousiers[5], utilize PBR (physically based rendering) in their rendering engines. For command PBR rendering, metallic / roughness (MR) and specular / glossiness (SG) workflows are the most popular pipeline. Based on quantitative analysis, four attributes are used to achieve complete description for materials.

### 1.2 Purpose

In this paper, we proposed a practical solution to restore the visual appearance of non-metallic materials by constructing their SVBRDF based on MR workflow with controllable light-bulb array and one camera. To proof the quality of PBR textures, the accuracy of BRDF from our device needs to be verified.

### 1.3 Target

In this study, we tested five textile samples that have a uniform surface structure and color. Finally, graphic reproductions are evaluated by verifying the data with the IS-SA (Imaging Sphere for Scatter and Appearance

Measurement) of Radiant Imaging Inc.. IS-SA is shown in Fig. 1. It utilizes a curved mirror as a hemi-spherical to capture the BRDF data under a high angular resolution (almost  $1^\circ$  for one illumination direction). Our SVBRDF measurement device is shown in Fig 2. The picture shows that our system combines a high-resolution camera and multi-direction illuminations.

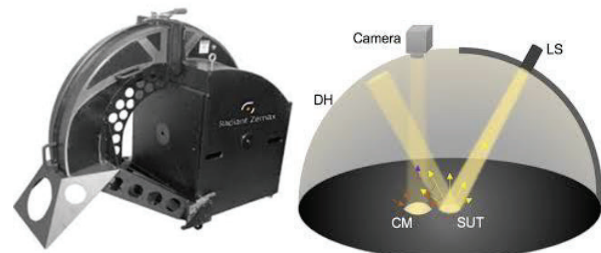


Fig. 1 IS-SA device of Radiant Imaging Inc. and schematic for capturing BRDF

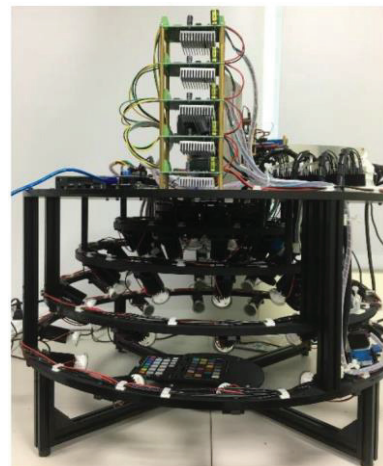


Fig. 2 Proposed SVBRDF System

## 2 EXPERIMENT

IS-SA device of Radiant Imaging Inc. is designed for BRDF measurement; Their dimensions only consider input angles ( $\varphi_{input}$ ,  $\theta_{input}$ ), output angle ( $\varphi_{out}$ ,  $\theta_{out}$ ) and luminance. However, SVBRDF data involve four parameters ( $x$ ,  $y$ ,  $\varphi$ ,  $\theta$ ) for each pixel on one image. Therefore, in our configuration, we reduce the order as a homogeneous sample. Because only BRDF needs to be discussed in this study. The five uniform textile samples have been tested in this study: Deepblue, Bluegreen,

Red, Beige, and Yellow.

### 2.1 PBR Texture Information Capture System

The SVBRDF measurement system, which was carried out in our previous work [6], can capture the SVBRDF information of texture samples with 55 multi-illuminate directions and retrieve the diffuse light and specular light responses for calculating the texture map with Cook-Torrance model. Fig. 3 shows the controllable light-bulb from various directions, and how SVBRDF obtained in progress.

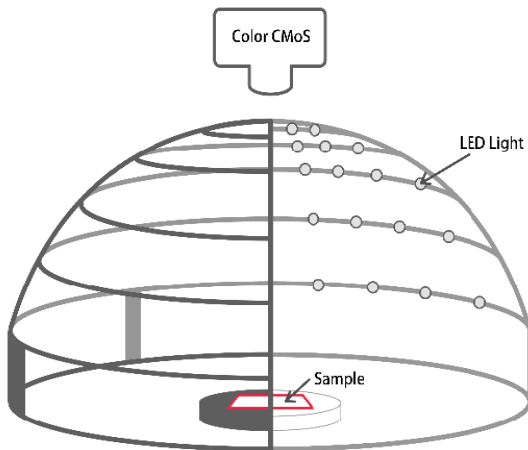


Fig. 3 Schematic draw of proposed SVBRDF System

### 2.2 PBR Texture Calculation

The PBR texture was calculated with Cook-Torrance model and the metallic / roughness (MR) workflow was used. Our study only focuses on non-metallic material. So there are only three types of PBR texture map should be calculated: base color map (as well as albedo), normal map, and roughness map. The metallic map is considered as empty data.

The base color map is recorded two types of information: the color of diffuse light and metal reflection of the material. In this study, the SVBRDF measurement system separates the diffuse color with the polarized light illumination. [7]

The normal map is usually stored as regular RGB images to represent to the surface normal vector as well as X, Y, and Z coordinates, respectively. In this study, the photometric stereo method is used to calculate the normal map. The photometric stereo method had been proposed by Woodham in 1980 [8]. Woodham's method is based on the orthogonal projection system. However, lots of image capturing systems are based on perspective projection in the real world. To overcome this problem, Tankus and Papadhimitri proposed the solution which is based on the perspective projection systems [9-10]. In this study, the SVBRDF measurement system used the photometric stereo method to calculate the normal map with the separating specular light information.

The roughness map controls how rough or how smooth

the texture's surface is. Rough texture scatters reflected light in more directions than smooth texture. The index of roughness is considered as a normalized value from 0, as ideal smooth, to 255 (ideal diffusion). In this study, the different roughness values were substituted into the Cook-Torrance model and calculate the error between the specular information and the roughness map. The roughness value of smallest error is recorded in the roughness map.

### 2.3 BRDF Measurement system IS-SA

"Imaging Sphere for Scatter and Appearance Measurement"(IS-SA) of Radiant Imaging Inc. provides rapid and comprehensive measurement of scattering distribution functions for materials [11]. The optical elements of the IS-SA and the basic theorem of BRDF information is shown as Fig. 4. It includes an imaging colorimeter and a hemispherical measurement chamber to capture BRDF information. Fig. 5 shows the schematic process of IS-SA. The parallel light (controllable angle) hits the surface and the reflection light distribute on the hemispherical measurement chamber. Again, the imaging colorimeter captures the image on the mirror which reflects the whole image of chamber, and then calculate the BRDF information for test samples.

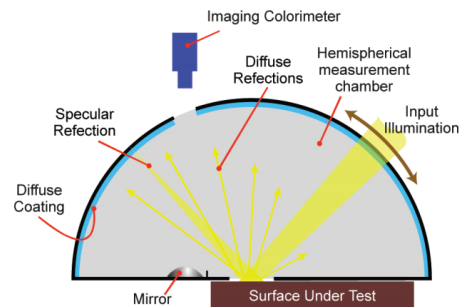


Fig. 4 Main optical elements of IS-SA

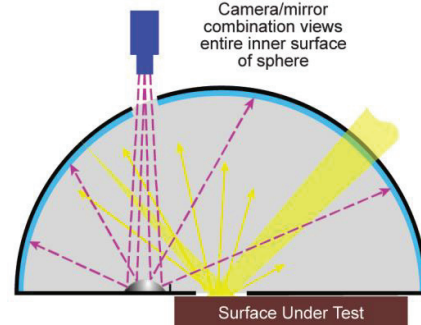


Fig. 5 Basic process of IS-SA

## 3 RESULTS

The five textile samples were measured by both of proposed SVBRDF device and IS-SA device. Because IS-SA can only measure the BRDF information. To verify our SVBRDF device, the texture maps of SVBRDF, normal map and roughness map, are averaged to be a single value to be substituted into the Cook-Torrance

model to calculate the BRDF. All results are normalized, and normalized cross-correlations (NCC) of them are calculated.

### 3.1 Deepblue textile

The result of deepblue textile is shown in Fig.6. The NCC between the ISSA and CT-Model of illuminating angle  $15^\circ$ ,  $30^\circ$ ,  $45^\circ$ ,  $60^\circ$ , and  $75^\circ$  are -0.22, 0.79, 0.76, 0.98, and 0.99.

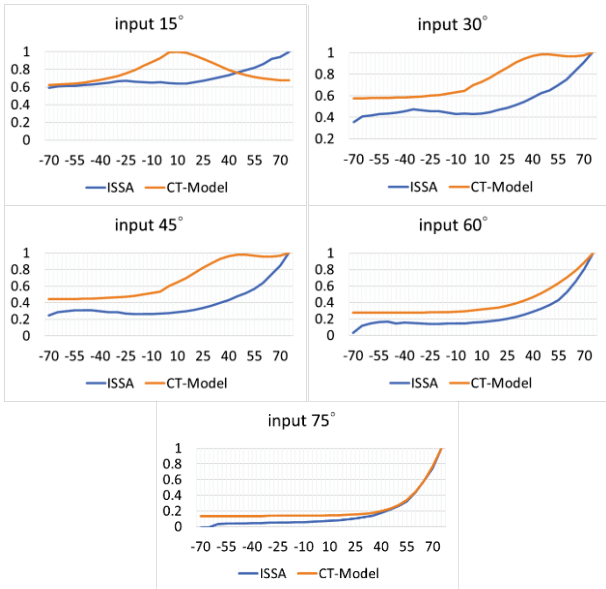


Fig.6 Result of Blue-Green textile

### 3.2 Blue-Green textile

The result of Blue-Green textile is shown in Fig.7. The NCC between the ISSA and CT-Model of illuminating angle  $15^\circ$ ,  $30^\circ$ ,  $45^\circ$ ,  $60^\circ$ , and  $75^\circ$  are -0.75, -0.23, 0.55, 0.97, and 0.99.

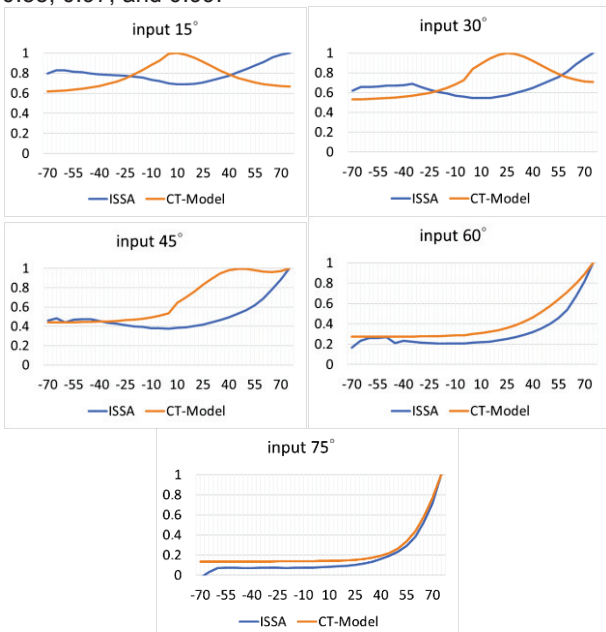


Fig.7 Result of Deep-Blue textile

### 3.3 Red textile

The result of Red textile is shown in Fig.8. The NCC between the ISSA and CT-Model of illuminating angle  $15^\circ$ ,  $30^\circ$ ,  $45^\circ$ ,  $60^\circ$ , and  $75^\circ$  are -0.52, -0.65, 0.41, 0.91, and 0.92.

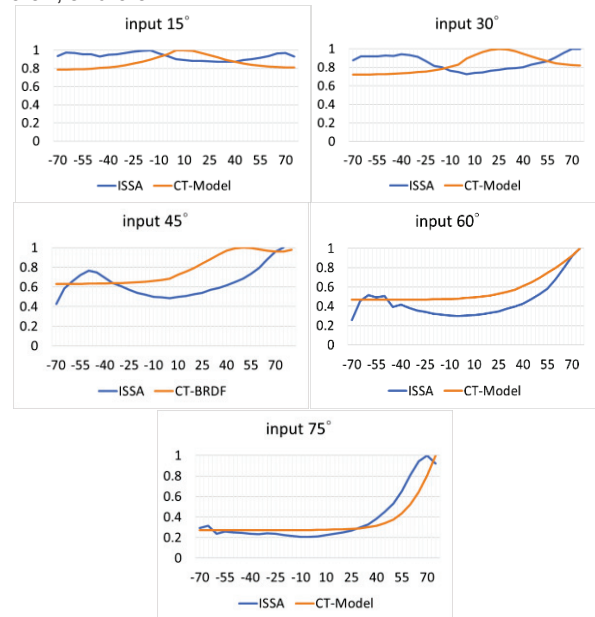


Fig.8 Result of Red textile

### 3.4 Beige textile

The result of Beige textile is shown in Fig.9. The NCC between the ISSA and CT-Model of illuminating angle  $15^\circ$ ,  $30^\circ$ ,  $45^\circ$ ,  $60^\circ$ , and  $75^\circ$  are -0.76, 0.11, 0.47, 0.89, and 0.99.

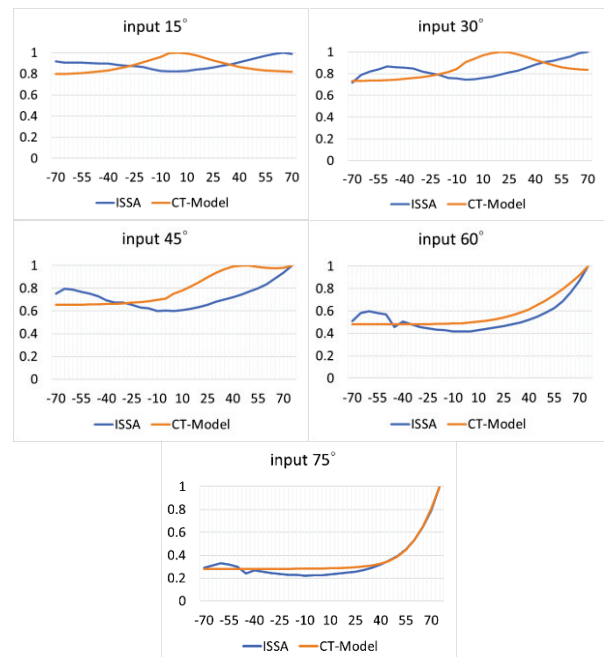


Fig.9 Result of Beige textile

### 3.5 Yellow textile

The result of Yellow textile is shown in Fig.10. The

NCC between the ISSA and CT-Model of illuminating angle  $15^\circ$ ,  $30^\circ$ ,  $45^\circ$ ,  $60^\circ$ , and  $75^\circ$  are 0.54, 0.72, 0.91, 0.99, and 0.99.

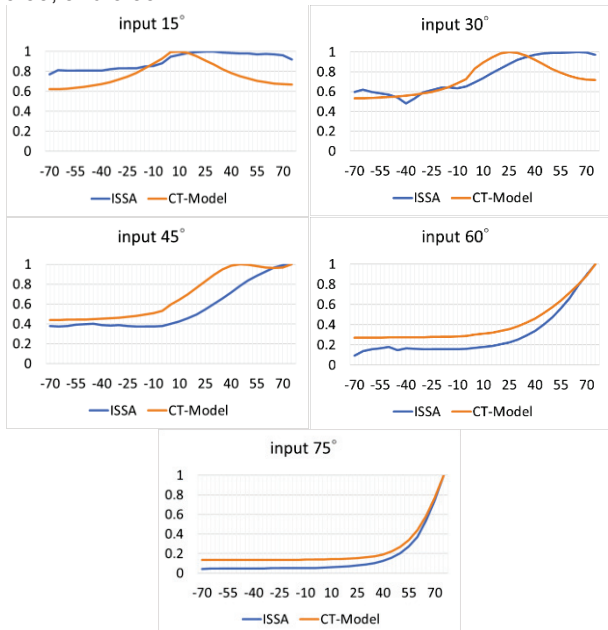


Fig.10 Result of Yellow textile

#### 4 DISCUSSION

The results are discussed by comparing with different illuminating angles and different textile samples.

##### 4.1 Influences of illuminating angles

According to the results, all samples' NCC of illuminating angle  $60^\circ$  and  $70^\circ$  are higher than 0.90. That means CT-Model has a good prediction in larger input angle. However, the results of NCC are much lower at the illuminate angle  $15^\circ$ ,  $30^\circ$ , and  $45^\circ$  (some of them are negative). Based on the IS-SA's results, specular light angles of almost samples are larger than the illuminating angle (except the yellow sample). We think that the light may go into the textile and make the specular angle much lager.

##### 4.2 Discission with different textile samples

The Yellow sample is only one that NCC results of all illuminating angles are positive. Fig. 10 shows that the specular angles are much equivalent to the illuminating angle and the prediction of CT-Model is much precisely.

#### 5 CONCLUSIONS

The BRDF information of five textile samples was measured by IS-SA and our SVBRDF devices. The results of our device are similar to the results of the benchmark device IS-SA when the illuminating angle is  $60^\circ$  and  $75^\circ$  based on CT-model. And, the result of yellow textile sample is the most similar to the result of IS-SA.

#### REFERENCES

[1] CIE, Commission Internationale de'Eclairage,

<http://www.cie.co.at/>

- [2] B. Burley and WaltDisneyAnimationStudios, "Physically-based shading at Disney," The ACM Special Interest Group on Computer Graphics, pp. 1–26, 2012.
- [3] C. Hery, R. Villemin, and P. Studios, "Physically based lighting at Pixar," Phys. Based on Shading Theory Pract. The ACM Special Interest Group on Computer Graphic Courses, pp. 1–23, 2013.
- [4] A. Prankevičius, "Physically based shading in Unity," Game Developers Conference, 2014.
- [5] S'ébastien Lagarde, Charles de Rousiers, "Moving Frostbite to Physically Based Rendering 3.0," SIGGRAPH 2014
- [6] Yu-Lun Liu, "Study on Visual Appearance Acquisition of Non-metallic Material Based on Sparse SVBRDF," Ph.D. Thesis, Institute of Applied Science and Technology, National Taiwan University of Science and Technology, 2018.
- [7] Wolff, Lawrence B. "Using polarization to separate reflection components." Proceedings CVPR'89: IEEE Computer Society Conference on Computer Vision and Pattern Recognition. IEEE, 1989.
- [8] R. J.Woodham, "Photometric Method For Determining Surface Orientation From Multiple Images," Opt. Eng., vol. 19, no. 1, pp. 139–144, 1980.
- [9] A.Tankus andN.Kiryati, "Photometric Stereo under Perspective Projection 3 . Background : The Image Irradiance," Int. Conf. Comput. Vis., vol. 1, pp. 611–616, 2005.
- [10] T.Papadhimitri andP.Favaro, "A new perspective on uncalibrated photometric stereo," IEEE Comput. Soc. Conf. Comput. Vis. Pattern Recognit., pp. 1474–1481, 2013.
- [11] Radiant Vision Systems, "Application of Imaging Sphere for BSDF White paper," 2014